Astron. & Astrophys. 4, 378—386 (1970)

The Cygnus X Region. VI. A New 2695 MHz Continuum Survey

H. J. Wendker
Max-Planck-Institut für Radioastronomie, Bonn

Received August 19, revised November 3, 1969

A 2695 MHz continuum survey of the Cygnus X region was undertaken with the NRAO 140-ft telescope with an angular resolution of 11′. A reference frame was established relative to which all intensities were measured. The improved positional accuracy helped to identify the resolved sources more accurately with optical features than had been possible before. In most cases, the deviations between centers of radio and optical emission of the H II regions are too large to be explained by positional inaccuracy. The lack of known distances of the H II regions in this area allows only to derive their emission measures. From a comparison between radio and H_α emission the visual absorption is estimated in a few cases. For IC 1318a a pair of possibly exciting stars is suggested.

Key words: Cygnus X — radio continuum radiation — optical identifications

I. Introduction

The continuum emission of the Cygnus X region was analyzed by Wendker (1966, Paper I). But it was soon noticed that especially the positional accuracy was not sufficient for a detailed discussion of individual features and for comparison with optical data. Dickel, Wendker and Bieritz (1969, Paper V) outlined a method of how to derive distances of some nebulae by comparing radio and optical data. Therefore a new survey of the radio continuum emission of the whole area seemed desirable. It is the goal of the present study to provide the improved radio data. A reference frame was established in order to determine the absolute zero level as well as possible. The relation to optical features, like associations and clusters, is also investigated. As the radio emission of the whole area is nearly completely of thermal origin (at least for frequencies higher than 1 GHz, as derived in Paper I) no further spectral information is required.

The observations are presented in Section II. In Section III and IV the unresolved background radiation and the resolved sources are derived. Section V contains the optical identifications. The results are discussed in Section VI.

II. Observations and Results

The observations were carried out with the 140-ft telescope at the National Radio Astronomy Observatory in May, 1967. The antenna and receiver calibration were kindly provided by Altenhoff (1969). The calibration basically assumes for Vir A a flux density of 123 f.u. (1 f.u. = 10^{-26} Wm^{-2} Hz^{-1}) at 2695 MHz. Half power beamwidths (HPBW's) of the telescope were 10.6′ and 11.6′ in right ascension and declination, respectively. The rms-noise fluctuations of the receiver system were about 0.1 °K in T_b (brightness temperature) for a time constant of 1 sec. The E-vector of the beam pointed in the north-south direction.

The performance of the equipment was monitored by observing at regular time intervals the planetary nebula NGC 7027 which is a point source for the angular resolution of the present survey.

After correcting the positions for instrumental effects, a mean positional error of each observed point of 1′ is adopted as a conservative estimate. From the rms-error of the intensity scale given as 5% by Altenhoff (1969) and the rms-scatter of the measured peak intensity of the monitoring source around its average value a mean error of 6% is adopted for the observed intensity. Both errors imply a significant improvement as compared with previous surveys which had positional errors of about 5′ and whose error of the intensities was of the order of 15%.

The area surveyed lies between 38°.5 and 44°.5 in declination and between 20^h08^m and 20^h45^m in right ascension. A necessary reference frame is provided by observing a set of four scans near the periphery of this area which extended far out. From these frame scans the brightness temperature values of their four

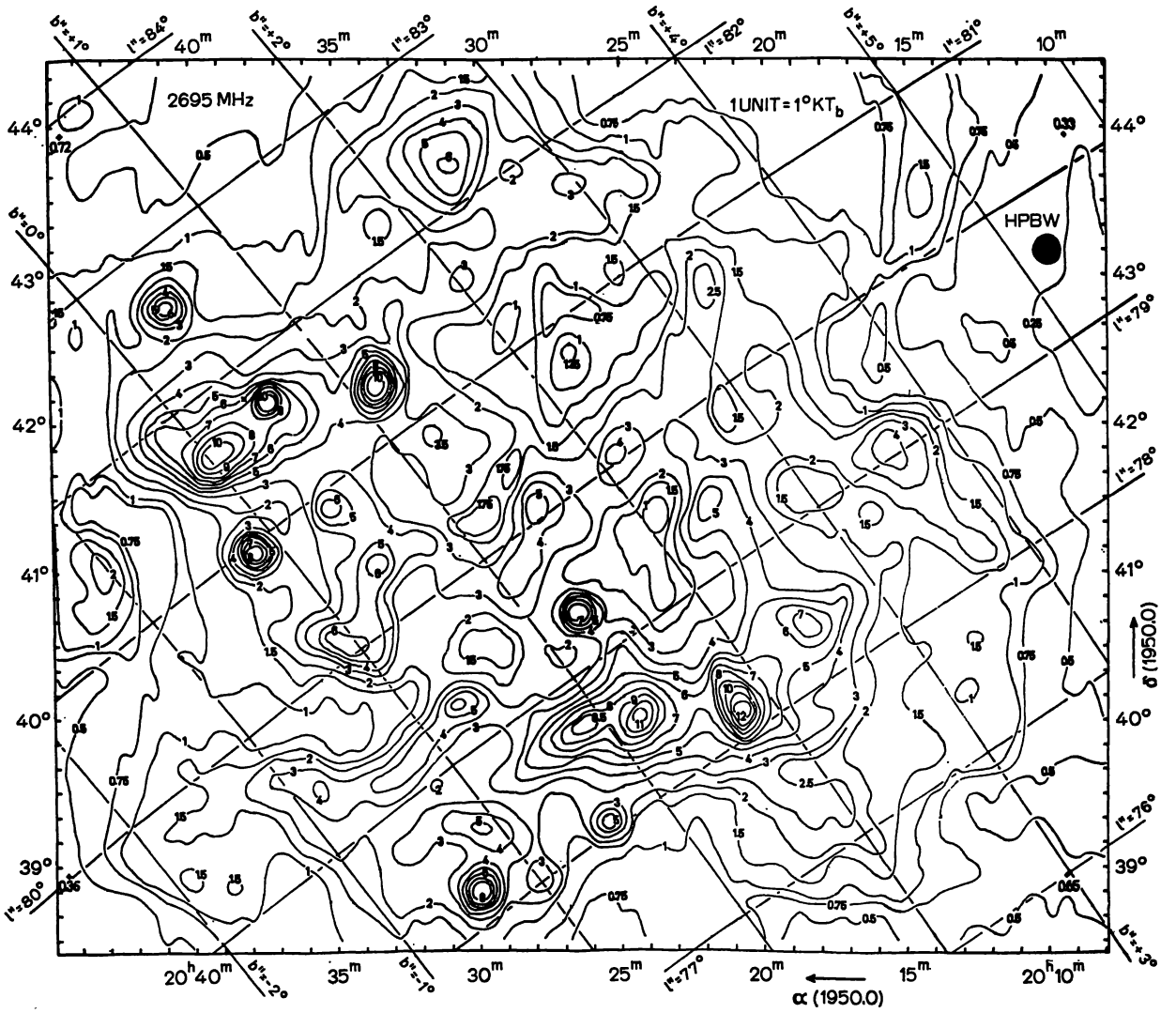

Fig. 1. Contour map of the Cygnus X region at 2695 MHz. The contours are normally spaced 1 °K T_b, but intermediate contours have been added for clarity where appropriate. A course grid of galactic coordinates (l^{II}, b^{II}) is indicated

Table 1. *The brightness temperature of the reference points*

α (1950.0)	δ (1950.0)	T_b (°K)
20h09m24s	+39°56'.8	0.56
09 28	43 56.8	0.34
44 28	39 56.1	0.36
44 31	43 56.1	0.72

cross-over points were determined and taken as reference point for the actual survey. Their values are listed in Table 1.

The internal error of the reference points is derived to be 0.05 °K T_b. However, it is impossible to assess any absolute errors of the reference frame. If a systematic error exists at all, it is obvious that the adopted values would be too low because the intensity of the galactic wings had been underestimated.

The survey was then carried out by observing declination scans from 38°.5 to 44°.5 about half a beamwidth apart in right ascension (about 26s) at a rate of 1°/min. At least two scans were averaged. A preliminary baseline was determined by averaging the first 10 values on each side of a cross-section. In a second step, the cross-sections were then fitted into the reference frame.

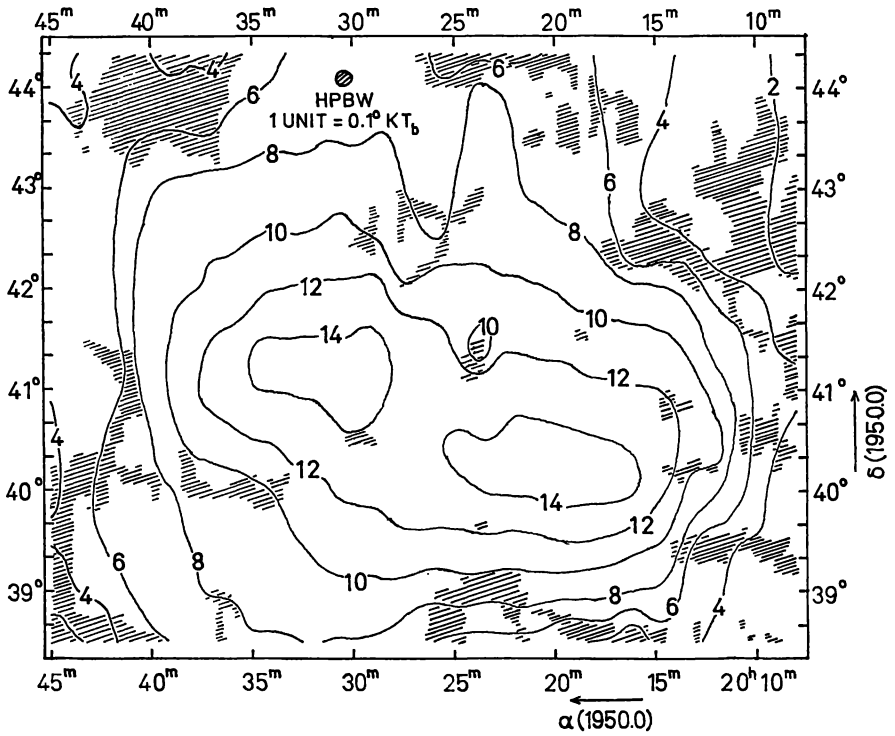

Fig. 2. Contour map of the unresolved background component of the Cygnus X region. The hatched areas are those where the unresolved component agrees with the total observed intensity of Fig. 1

From the cross-sections a contour map was drawn with isophotes of equal brightness temperature. This contour map is presented in Fig. 1. The integrated total flux density represented by the contour map is 5390 f.u.

III. The Unresolved Background Component

In surveys of the galactic continuum radiation it is desirable to separate sources from the unresolved background component. At present there exists no generally accepted procedure for this separation which, consequently, is always somewhat arbitrary. Here, the separation is based on a stacking procedure described e.g. by Altenhoff (1968). Every five adjacent cross-sections were stacked and their lower envelope was adopted as the unresolved background for the center cross-section. Then, background cross-sections with constant declination were constructed. These showed that small ridges appeared in some areas up to two or three beamwidths wide only. These ridges were smoothed out manually.

The unresolved component thus obtained is shown in the contour map of Fig. 2. The hatched areas are those where the originally observed intensity agrees with that of the unresolved component. The unresolved background seems to have just two components which fit all the deeper minima of the map of Fig. 1. It may be that, with increased resolution, the maxima of the unresolved background will disappear. The only "small scale irregularity" is in the 0.8 °K contour line in the north of the map, but there seems to be no way to avoid it.

In Paper I it was shown that the unresolved background component is of thermal origin or at least that the amount of non-thermal radiation is negligible for frequencies higher than 1 GHz. In this connection, it is of interest to note that the western maximum of the unresolved component of the map in Fig. 2 coincides with the area where there seems to be also a general optical background radiation in H_α as seen on the H_α-photographs used in Paper V. The other maximum is behind the Great Cygnus Rift and no optical comparison is possible.

The integrated flux density of the unresolved background component is 2260 f.u. or 42% of the total observed intensity.

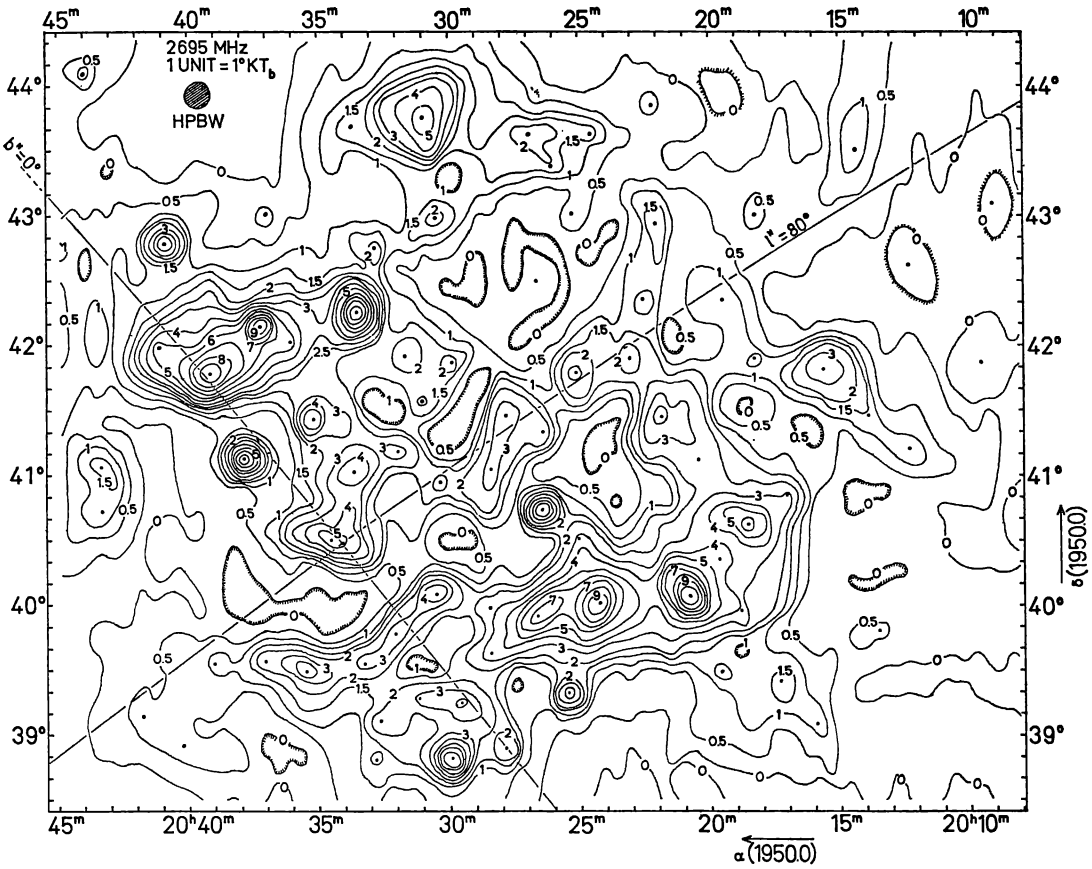

Fig. 3. Contour map of the resolved components (map of Fig. 1 minus map of Fig. 2). The resolved sources of Table 2 are indicated by dots

IV. The Resolved Sources

The unresolved component of the emission was subtracted from the observed distribution. This difference is also shown as a contour map in Fig. 3. Owing to the high complexity of the whole area, it only seems possible to obtain more informations on the most prominent emission features. For the same reason and as no better distribution function for sources is known, it is certainly appropriate to approximate the sources by gaussians. Therefore, it was tried to decompose the most prominent features in gaussian sources.

The gaussians were fitted to the observed maxima and well-defined shoulders in two perpendicular directions (right ascension and declination). In this way, 78 well-defined sources were obtained. This number roughly means two sources per square degree. The source G 81.7 + 0.5 (= DR 21) was not derived in such a manner. For this source, the flux density was adopted from the spectrum given by Mezger *et al.* (1967), and a point source of this intensity subtracted from the observed distribution before the gaussian fit was made.

The center position, the maximum observed brightness temperature $T_{b\max}$ and the observed HPW, Θ'_α and Θ'_δ, were directly obtained from the gaussian fits. The flux density S_{2695} of each source was calculated from the last two parameters according to the well known formula:

$$S_{2695} = 2\,k\,\lambda^{-2}\,T_{b\max}\,\Omega\,, \qquad (1)$$

where Ω is the solid angle of the gaussian, k the Boltzmann constant and λ the wavelength. The sources are listed in Table 2. The first to fifth columns have the following meaning: the designation (G-number) of the source, the equatorial coordinates for the epoch 1950.0, the maximum observed brightness temperature $T_{b\max}$, the HPW's, Θ_α and Θ_δ, corrected for the beam size and the flux density. The

Table 2. *The source catalogue*

Source	α(1950.0) 20^h+	δ(1950.0)	$T_{b\,max}$ (°K)	$\Theta_\alpha \times \Theta_\delta$	S_{2695} (f. u.)	E (cm^{-6} pc)	Identification
G 76.8+2.0	$15^m.95$	+39°05′	1.10	15′×28′	13.0	2990	34
G 77.1+2.8	13.50	39 48	0.60	54×14	12.8	1630	41
G 77.2+2.0	17.35	39 25	1.60	21×29	25.1	3980	40
G 77.6+1.6	19.70	39 29	1.60	20×20	17.9	4330	49
G 77.8+2.0	18.85	39 57	3.00	16×16	24.3	9150	51
G 78.0+0.0	27.95	38 54	3.00	12×13	17.9	11060	Rift
G 78.1+0.6	25.50	39 20	4.55	9×7	18.5	28330	67, S of IC1318c
G 78.2−0.4	29.95	38 49	8.10	11×12	44.2	32300	Rift
G 78.2+1.8	20.85	40 04	11.10	21×21	133.9	29270	63, γ Cygni source
G 78.2+3.8	12.30	41 12	1.25	20×21	14.5	3340	59
G 78.3+2.1	19.65	40 21	2.70	25×14	28.5	7850	64
G 78.4+2.5	18.55	40 37	6.20	25×21	86.3	15860	E of 68
G 78.4+2.8	17.05	40 51	2.35	13×14	14.8	7850	NW of 68
G 78.5−0.8	32.85	38 48	1.55	15× 8	8.6	6920	Rift
G 78.5−0.1	29.60	39 15	4.05	19×16	37.2	11800	Rift
G 78.5+1.2	24.30	40 01	9.70	20×31	155.2	24140	70/71/72, IC1318b
G 78.5+4.6	09.55	41 52	0.25	17×20	2.5	700	74
G 78.6+3.6	13.90	41 27	1.40	14×19	11.7	4240	78
G 78.7−0.6	32.65	39 07	2.40	11×16	15.5	8480	Rift
G 78.7−0.3	31.15	39 17	2.50	14×16	18.5	7970	Rift
G 78.7+0.4	28.40	39 38	3.20	15×14	22.9	10530	S of 76
G 78.7+0.8	26.70	39 55	7.30	24×20	94.6	19010	76
G 78.9+0.5	28.65	39 59	2.25	10×12	11.7	9390	faint extension of IC 1318c
G 79.0+1.4	25.10	40 31	2.80	12×18	20.5	9150	81
G 79.0+2.5	20.40	41 07	2.75	22×32	48.8	6700	84
G 79.0+3.6	15.60	41 49	3.60	28×20	53.3	9190	83, IC 1318a
G 79.1−0.5	33.30	39 32	3.05	25×14	32.2	8880	Rift
G 79.2−0.1	32.10	39 47	3.50	12×14	21.8	12500	85
G 79.3+0.3	30.50	40 05	5.00	17×11	34.3	17700	faint knot of Hα
G 79.3+1.3	26.45	40 44	6.55	9×8	27.5	36830	86
G 79.4−0.8	35.55	39 29	3.15	15×16	24.4	9810	Rift
G 79.4+2.4	21.80	41 27	4.30	20×32	70.7	10650	88
G 79.4+3.2	18.70	41 54	1.50	12×16	9.8	4920	89
G 79.4+4.5	12.30	42 37	0.25	11×10	1.3	1130	90
G 79.4+5.3	09.00	43 06	0.15	5×15	0.7	910	91
G 79.5−1.9	40.30	38 55	0.95	20×16	9.1	2740	faint Hα
G 79.6−1.0	37.10	39 34	2.30	11×16	14.8	8120	Rift
G 79.8−1.3	39.05	39 33	1.10	20×21	12.8	2950	Rift
G 79.8+1.2	28.40	41 03	3.50	17×16	29.6	10490	96
G 79.8+1.7	26.45	41 20	2.05	10×16	12.6	7600	97
G 79.9−2.0	41.80	39 09	0.75	15×19	6.6	2220	faint Hα
G 79.9+2.5	23.10	41 54	2.35	17×26	28.6	6240	NW of 100
G 79.9+3.3	19.50	42 21	1.35	19×36	23.7	3340	98
G 80.0+0.8	30.50	40 57	2.10	16×16	17.0	6410	faint knot of Hα
G 80.0+2.1	25.15	41 47	3.15	13×22	28.1	9480	E of 100
G 80.1−0.1	34.55	40 30	5.25	32×13	66.0	15310	102
G 80.1+1.5	27.85	41 28	4.05	12×22	34.5	12610	104
G 80.2+2.8	22.55	42 21	1.55	22×19	18.0	4160	114
G 80.3+0.8	31.95	41 12	3.25	17×14	25.3	10260	faint Hα
G 80.3+3.9	18.30	43 00	0.60	17×27	7.5	1570	117

Table 2 (continued)

Source	α(1950.0) 20^h+	δ(1950.0)	$T_{b\max}$ (°K)	$\Theta_\alpha \times \Theta_\delta$	S_{2695} (f. u.)	E (cm^{-6} pc)	Identification.
G 80.3+4.7	$14^m.35$	+43°30′	1.35	15′×31′	17.5	3630	111/118/119/HS 191
G 80.4+0.4	33.70	41 02	5.00	17×22	53.2	13720	140
G 80.5+1.1	31.00	41 34	2.05	14×16	15.2	6550	112
G 80.6+1.5	29.80	41 53	2.20	14×15	15.7	7210	faint Hα
G 80.7+3.3	22.10	42 56	1.95	10×30	19.5	6260	121/124
G 80.8+0.4	35.10	41 26	5.10	17×16	43.2	15330	
G 80.8+2.3	26.70	42 30	0.40	8×13	2.0	1850	faint Hα
G 80.9−0.2	37.80	41 08	7.20	9×8	30.2	40460	
G 80.9+1.2	31.70	41 55	2.25	21×21	27.1	5930	faint Hα
G 81.1+2.8	25.25	43 01	0.75	14×14	5.1	2510	130
G 81.3−1.2	43.30	40 43	1.25	15×18	10.5	3750	
G 81.4+1.2	33.50	42 16	9.55	14×21	85.9	28180	140
G 81.4+2.9	26.10	43 23	1.40	19×8	9.2	5830	134
G 81.4+3.8	22.15	43 51	0.55	23×16	5.9	1550	135
G 81.5−1.0	43.30	41 04	1.65	16×16	13.4	5050	faint Hα
G 81.5+0.6	36.10	42 02	5.45	22×25	78.4	13740	140 (?)
G 81.5+1.9	30.45	42 49	2.30	17×16	19.5	6920	
G 81.5+3.3	24.60	43 37	1.50	19×14	12.7	4610	137
G 81.6+0.0	39.15	41 47	10.00	25×20	134.2	25890	
G 81.7+0.5	37.25	42 09	5.90	P	15.5	—	DR 21
G 81.7+1.6	32.85	42 45	2.30	14×19	19.2	6970	dark cloud
G 81.7+2.9	26.90	43 38	2.40	25×16	27.5	6630	NE of 134
G 82.0−0.1	41.15	41 59	4.80	18×25	59.0	12650	
G 82.3+1.1	37.00	43 01	0.55	19×16	5.1	1630	
G 82.3+2.4	31.00	43 46	5.40	23×34	104.9	12940	155
G 82.5+2.0	33.70	43 42	1.80	26×26	30.7	4390	157
G 82.6+0.4	40.90	42 47	5.75	10×8	25.3	30510	knot of Hα
G 84.0+0.8	44.00	44 06	1.20	3×5	3.6	23150	W of NGC 7000

center positions of the sources are also shown as dots in Fig. 3.

The total flux density of all sources is about 2400 f.u., i.e. only 44% of the total flux density observed or 76% after the background has been substracted.

As the distances of the sources are not yet available, distance dependent parameters are not derived in this paper. The only meaningful parameter which can be calculated is the emission measure E of the center of the source. For this purpose, the observed brightness temperature of the source center $T_{b\max}$ was corrected for beam smoothing and E calculated according to:

$$E\ (\mathrm{cm}^{-6}\ \mathrm{pc}) = 2060\ T_b\,, \qquad (2)$$

a relation derived in Paper V and valid for this frequency. It assumes an electron temperature of 6000 °K for the H II region. E is listed in column 7 of Table 2.

V. Optical Identifications

From earlier surveys it was derived that all sources, except the so-called γ Cygni source, G78.2+1.8, and perhaps also G78.4+2.5, have a thermal spectrum. In a search for corresponding optically visible H II regions the catalogue of H_α emission nebulae by Dickel, Wendker and Bieritz (1969) was used for identification. In the few cases where the area was not covered by the plates from which the catalogue was compiled, the red prints of the National Geographic Society - Palomar Observatory Sky Survey were searched for traces of H_α emission. The results are listed in column 8 of Table 2. The numbers are those of the catalogue by Dickel, Wendker and Bieritz. It is also indicated there if faint and uncatalogued H_α emission is present at the source position. Several sources are in the area which is very heavily obscured by the Great Cygnus Rift.

Here the absorption is so high that an identification seems to be completely hopeless. This fact is denoted "Rift" in column 8. In addition, a few well known notations are also given.

The statistics read as follows:

44 sources are identified with entries in the above catalogue;

15 are in areas where faint H_α is present;

11 are behind the Rift and

8 have no relation to any optical feature.

During the identification procedure it was noted that in nearly all cases the centers of the optical and radio emission do not coincide but are in general about 5 to 10′ apart. Normally, their angular sizes are much larger than 10′ and thus their areas overlap to quite an extent. Therefore their identifications appear to be justified. It is certain that this effect is not due to positional inaccuracies, which were shown above to be in the order of 1′ or less. This point will be discussed further in the next section.

A new search was undertaken for possible exciting stars of these H II regions. The positions and HPW's of the radio sources were used together with the Luminous Star catalogue of OB stars (Hardorp, Theile and Voigt, 1964). The search turned out to be nearly completely negative. The OB stars seem to avoid source areas. There is one exception. This is G79.0+3.6 or the well known nebula IC 1318a for which, to the author's knowledge, no exciting star is known. There are two stars classified OB^+ and OB, about 3′ away from the radio center. Their designation in the catalogue is LS III + 41°14 and LS III + 41°15 (= BD + 41°3689). It is suggested that one or both of these two stars are the exciting stars of IC 1318a.

From the optical appearance of IC 1318a it is clear that the two stars must undergo more absorption than the brightest optical part of the nebula which is about 4′ south of the two stars. A very rough estimate is that, at the position of the stars, there are at least 2 magnitudes more of absorption. For the optical center a visual absorption of $A_v \approx 2^m.5$ was derived in Paper V. Assuming that the star LS III + 41°14 has an absolute visual magnitude about $M_v \approx -6$, a distance modulus of DM ≈ 11 is derived which compares well with the distance estimated in Paper V. This very rough estimate cannot be proved until more precise observations are available.

There are four more stars in the catalogue which fall inside the halfwidth ellipse of a radio source. However, they are not only fairly far away from the center position but also classified as OB^-, which means that they are most probably middle or perhaps early B stars. These facts do not make them very suitable candidates for exciting stars.

VI. Discussion

In the previous sections new observations of the radio continuum of the Cygnus X region were presented. As only the accuracy of the observations and not the resolution was significantly improved, the overall radio appearance of the area is not changed drastically but is similar to that of the surveys by Pike and Drake (1964), Downes and Rinehart (1966) and those of Paper I. The previous conclusion that Cygnus X represents a region of high natural and projectional clumping is certainly not changed. The fainter and smaller features, however, can be regarded as more reliable due to the increased accuracy of positions and intensity. In this connection, attention is drawn to subfeatures of the area which were not noticed earlier.

First, all pronounced minima of the map lie on lines of generally lower intensity. All such "dip-lines" originate in the area around $\alpha = 20^h30^m$ and $\delta = 41°$. Second, several small and elongated ridges are visible on the map. The two most prominent ridges are centered at about $\alpha = 20^h29^m$, $\delta = 41°$ and $\alpha = 20^h31^m$, $\delta = 39°.5$. They show hardly any sign of being resolved into components.

In Section V attention was drawn to the fact that optical and radio centers do not coincide very well. This apparently means that the optical appearance of the H II regions is governed to a high degree by the distribution pattern of the absorbing material. If we take the radio centers for the real ones, it seems that real centers of the H II regions in the Cygnus area are more obscured than their outskirts. The first conclusion is also supported by the fact that the high ellipticities found for the H_α emission nebulae by Dickel, Wendker and Bieritz (1969) do not appear in the dimensions of the radio sources. In the latter, hardly any source has an axis ratio greater than two, while more than three quarters of the nebulae have axis ratios exceeding two.

There may be two reasons for not finding more exciting stars. First, the H II regions may be in an early stage of evolution and their exciting stars are still hidden in the surrounding dust (see e.g. Schraml and Mezger, 1969). Second, it may simply be that the limiting magnitude for the search of the early type stars was not yet sufficiently low, because high absorption values are known to occur in the Cygnus X

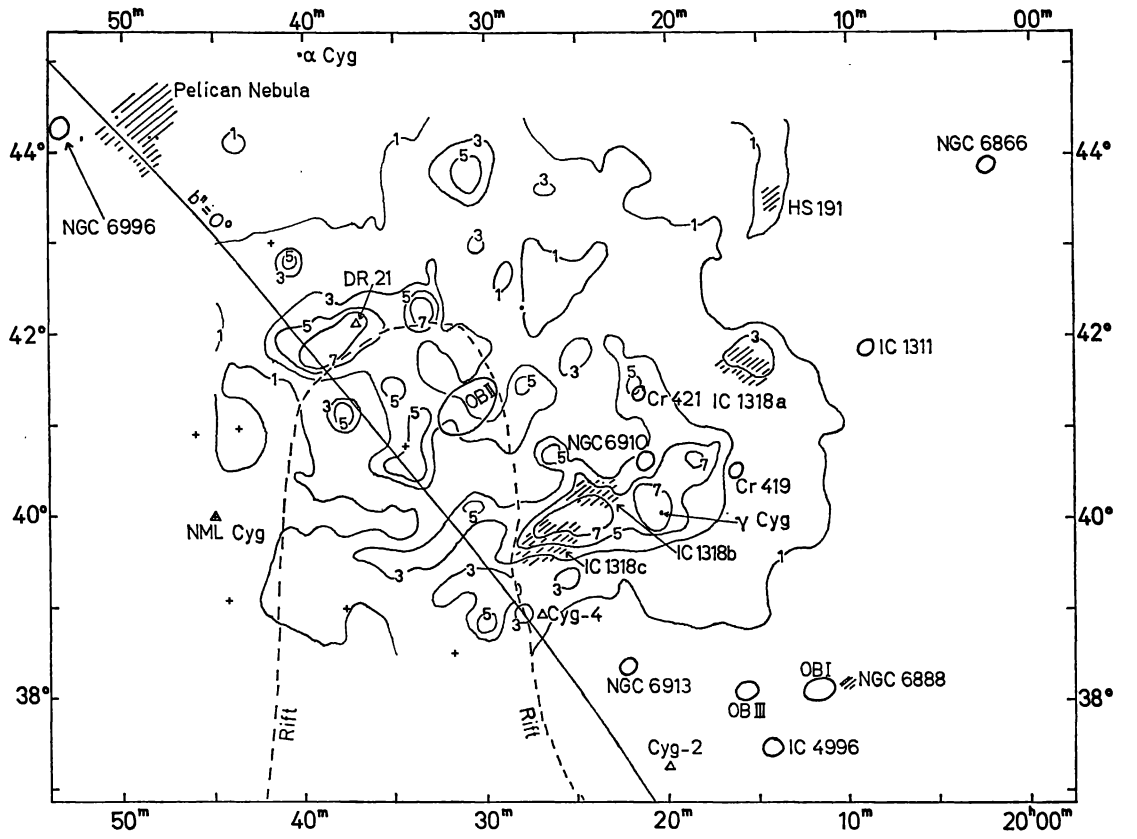

Fig. 4. Sketch of the Cygnus X region and surrounding area. The contour lines are from Fig. 1 in °K T_b. The big circles indicate open clusters and associations (Alter, Ruprecht and Vanysek, 1958), the hatched areas the brightest H_α emission nebulae, the dots possible T Tauri stars (Herbig, 1962), the triangles OH emission centers (Elldér, Rönnäng and Winnberg, 1969) and the crosses infrared stars (Ackermann *et al.*, 1968; Ulrich *et al.*, 1966)

region. A good example for this latter reason obviously is IC 1318a (see Section V).

These conclusions are drawn from the appearance of the western and northern parts of the Cygnus X region. The eastern part is hidden behind the Great Cygnus Rift. The only extensive discussion of this foreground dark cloud seems to be that by Miller (1937). He comes to the conclusion that the Rift is between 0.5 and 1.6 kpc distance with a total absorption up to four magnitudes, For most H II regions in this area the absorption must be a few magnitudes higher in order to hide them optically.

There are seven sources which have high emission measures, lie more or less isolated and have a small diameter (10′ or less). For these sources, which look like spherical H II regions, the lower limit of the visual absorption can be estimated. From the H_α-photographs discussed in Paper V an upper limit can be placed on the apparent optical emission measure E'. The true emission measure is taken from Table 2, column 7. Then the visual absorption A_v can be calculated according to the formulae in Paper V. The results are listed in columns 1 to 3 of Table 3 where the source designations, E' and A_v are given. It is to be seen that the values of A_v are between 6 and 9 magnitudes. Thus these sources are estimated to be behind the Rift. Their distance would then be 2 kpc or more.

Table 3. *Visual absorption of isolated sources*

Source	E' (cm^{-6} pc)	A_v
G78.0 + 0.0	100	$6^m.5$
G78.1 + 0.6	300	6.3
G78.2 − 0.4	150	7.5
G79.3 + 1.3	450	6.1
G80.9 − 0.2	100	8.3
G81.4 + 1.2	100	7.8
G82.6 + 0.4	150	7.4

Nearly all known open clusters and associations of the Cygnus constellation are outside the area under discussion. This is illustrated in the sketch of Fig. 4. In it a few radio contours from the map of Fig. 1 are outlined. The positions of all known associations and clusters (Alter, Ruprecht and Vanysek, 1958) are indicated together with other features. The outline of the Rift is also drawn in. No correlation seems to exist between these objects and the radio emission. There are only two open clusters, NGC 6910 and Cr 421, and one association, Cyg OB II, inside the Cygnus X region. None of them shows up conspicuously in the radio contour map. NGC 6910 lies close to the very strong γ Cygni source. There is an asymmetry in the contours but it is too weak to allow a reliable decomposing. Cr 421 falls inside but near the edge of the half-power ellipse of the source G79.4+2, yet it is not obvious that an identification is permitted. The Cyg OB II association seems to be unrelated to a discrete radio source but lies in an area which is near an emission minimum. This was already pointed out by Pike and Drake (1964). From this fact, Wickramasinghe and Reddish (1968) concluded that the hydrogen of the association which is not yet used up for star formation exists in form of solid hydrogen mantles of grains. If the optical position and dimension are taken from Reddish, Lawrence and Pratt (1966), it is seen that the optical center of the association ($20^h30^m.9$; 41°13′) does not coincide with the emission minimum in the radio continuum but rather lies close to a weak ridge surrounding the source G80.0+0.8. This source and G80.3+0.8 occupy the southern half of the projected extension of Cyg OB II. Only the northern half is projected on an emission minimum. On the H_α-photographs (Paper V) there is faint emission in the whole area of the association. It is, therefore, suggested that H II is present in the association although it may be unexpectedly faint.

Acknowledgements. It is a pleasure to thank D. S. Heeschen, director, for granting the observing time and the staff of the National Radio Astronomy Observatory[1]) for assistance. This study was begun while the author was with the Vermilion River Observatory, and I wish to thank G. C. McVittie and G. W. Swenson Jr. for their hospitality and support. I am indebted to W. Altenhoff for supplying the information concerning the calibration and to J. Schraml for allowing to use his computer reduction program. Discussions with H. R. and J. R. Dickel helped to clarify problems. I also wish to thank O. Hachenberg for his encouragement and, last not least, P. G. Mezger for critical comments on the manuscript.

References

Ackermann, G., Fugmann, G., Hermann, W., Voelcker, K. 1968, *Z. Astrophys.* **69**, 130.
Altenhoff, W. 1969 (in preparation).
Altenhoff, W. 1968, in Interstellar Ionized Hydrogen, ed. Y. Terzian, New York, W. A. Benjamin, Inc. p. 519.
Alter, G., Ruprecht, J., Vanysek, V. 1958, Catalogue of Star Clusters and Associations, Publ. House Czech Acad. Sci. Prague.
Dickel, H. R., Wendker, H. J., Bieritz, J. H. 1969, *Astron. Astrophys.* **1**, 270 (Paper V).
Downes, D., Rinehart, R. 1966, *Astrophys. J.* **144**, 937.
Elldér, J., Rönnäng, B., Winnberg, A. 1969, *Nature* **222**, 67.
Hardorp, J., Theile, I., Voigt, H. H. 1964, Luminous Stars in the Northern Milky Way III, Hamburg-Bergedorf.
Herbig, G. H. 1962, *Adv. Astron. Astrophys.* **1**, 47.
Mezger, P. G., Altenhoff, W., Schraml, J., Burke, B. F., Reifenstein III, E. C., Wilson, T. L. 1967, *Astrophys. J.* **150**, L157.
Miller, F. D. 1937, *Annals Harvard College Obs.* **105**, 297.
Pike, E. M., Drake, F. D. 1964, *Astrophys. J.* **139**, 545.
Reddish, V. C., Lawrence, L. C., Pratt, N. M. 1966, *Publ. Roy. Obs. Edinburgh* **5**, 111.
Schraml, J., Mezger, P. G. 1969, *Astrophys. J.* **156**, 269.
Ulrich, B. T., Neugebauer, G., McCammon, D., Leighton, R. B., Hughes, E. E., Becklin, E. 1966, *Astrophys. J.* **146**, 288.
Wendker, H. J. 1966, *Mitt. Astr. Inst. Münster* Nr. 10 (Paper I).
Wickramasinghe, N. C., Reddish, V. C 1968, *Nature* **218**, 661.

H. J. Wendker
Max-Planck-Institut für Radioastronomie
BRD-5300 Bonn, Argelanderstr. 3, Germany

[1]) The National Radio Astronomy Observatory is operated by Associated Universities, Inc. under contract with the National Science Foundation.